

BRITTLE FRACTURE INITIATION CHARACTERISTICS  
UNDER BI-AXIAL LOADING

Y. Ueda\*, K. Ikeda\*\*, T. Yao\*, M. Aoki\*\*, T. Yoshie\* and T. Shirakura\*\*

## INTRODUCTION

In this paper, brittle fracture initiation characteristics of plate with an inclined notch subjected to bi-axial tension are investigated. The brittle fracture tests are conducted on the cruciform specimens at the load ratio of 1/1, 1/2 and 0/1, and also on straight side specimens under uni-axial tension.

Firstly, fracture tests of specimens of PMMA (polymethylmethacrylate) or a perfectly brittle material, are conducted and several existing fracture criteria are discussed from the test results. Then, tests of SM41 (mild steel) fractured in a semi-brittle manner, are also conducted, and the test results are compared with those of PMMA.

## EXISTING CRITERIA

As for the criteria of brittle fracture under mixed mode stress system, there are the following three main ones defined by: (1) the maximum tangential stress,  $\sigma_{\theta, \max}$ , proposed by Erdogan and Sih [1], and the modified one by Williams and Ewing [2], (2) the minimum strain energy density factor,  $S_{\min}$ , proposed by Sih [3] and (3) the maximum decreasing rate of total potential energy or the maximum crack extension force,  $G_{\theta, \max}$ , by Anderson et al [4]. In this chapter, these criteria will be reviewed briefly.

Maximum Tangential Stress Criterion

The tangential stress,  $\sigma_{\theta}$ , in the neighbourhood of the crack tip in Figure 1 can be expressed by

$$\sigma_{\theta} = \frac{a}{2\sqrt{2r}} \cos \frac{\theta}{2} \left[ \sigma_Y (1 + \cos \theta) - 3\tau_{XY} \sin \theta \right] + \sigma_X \sin^2 \theta + \sqrt{\frac{2r}{a}} F(\sigma_Y, \tau_{XY}, \theta) + \dots \quad (1)$$

where

$$\sigma_Y = \sigma_y^{\infty} \sin^2 \beta + \sigma_x^{\infty} \cos^2 \beta, \quad \sigma_X = \sigma_y^{\infty} \cos^2 \beta + \sigma_x^{\infty} \sin^2 \beta, \quad \tau_{XY} = \left( \sigma_y^{\infty} - \sigma_x^{\infty} \right) \sin \beta \cos \beta \quad (2)$$

In the above expression,

$$\sigma_x^{\infty} \text{ and } \sigma_y^{\infty} \quad : \text{ applied uniform stresses at infinity in the x and y directions, respectively}$$

\* Welding Research Institute of Osaka University.

\*\* Structural Engineering Laboratory, Kobe Steel, Limited, Japan.

$\sigma_X$ ,  $\sigma_Y$  and  $\tau_{XY}$  : resolved stress components of  $\sigma_x^\infty$  and  $\sigma_y^\infty$  with respect to the X-Y coordinates.

Using the first term in equation (1), Erdogan and Sih proposed the  $\sigma_{\theta, \max}$  criterion. It is restated that a crack will initiate when the maximum value of  $\sigma_\theta$  reaches some critical value as a material constant, that is,

$$\sigma_{\theta_0} \sqrt{2r} = \text{const.} \quad (3)$$

This direction,  $\theta = \theta_0$ , is determined from  $\partial\sigma_\theta/\partial\theta = 0$ , that is,

$$\sigma_Y \sin\theta_0 - \tau_{XY}(1 - 3 \cos\theta_0) = 0. \quad (4)$$

However, Cotterell [5] has discussed the inclusion of other terms with reference to crack direction under simple tension, and has concluded that the second term has a significant effect. Williams and Ewing also proposed the same criterion using the first two terms in equation (1). In this case, the direction of initial crack propagation is obtained from the following equation:

$$\sigma_Y \sin\theta_0 - \tau_{XY}(1 - 3 \cos\theta_0) - \frac{16}{3} \alpha \sigma_X \sin \frac{\theta_0}{2} \cos\theta_0 = 0 \quad (5)$$

where

$$\alpha = \sqrt{2r/a}. \quad (6)$$

When equation (5) is solved, the value of  $r$  should be given. Williams and Ewing maintain that their theoretical prediction is in good agreement with the test results when  $r$  is assumed to be 0.05 mm. However, the physical meaning of this value is not clear.

#### Minimum Strain Energy Density Factor Criterion

The amount of strain energy,  $dW$ , stored in an infinitesimal element,  $dA$ , in the neighbourhood of the crack tip, is given by

$$dW = \frac{1}{\pi r} (a_{11}K_I^2 + 2a_{12}K_I K_{II} + a_{22}K_{II}^2) dA \quad (7)$$

where the constants  $a_{ij}$  ( $i, j = 1, 2$ ) are functions of  $\theta$  and material properties. The strain energy density factor (S.E.D.F.),  $S$ , is defined as

$$S = \frac{1}{\pi} (a_{11}K_I^2 + 2a_{12}K_I K_{II} + a_{22}K_{II}^2). \quad (8)$$

The minimum strain energy density factor,  $S_{\min}$ , criterion is restated that a crack will initiate in the direction of minimum S.E.D.F. when  $S_{\min}$  reaches a critical value,  $S_{cr}$ , which is a material constant,

$$S_{\min} = S_{cr}. \quad (9)$$

However, the physical background of this criterion should be discussed in future.

#### Maximum Decreasing Rate of Total Potential Energy Criterion

The maximum decreasing rate of total potential energy,  $G_{\theta, \max}$ , criterion is restated as follows: a crack will initiate in the direction of the maximum value of  $G_\theta$ , which is the decreasing rate of the total potential energy, when  $G_{\theta, \max}$  reaches a critical value,  $G_{cr}$ , which is a material constant, that is,

$$G_{\theta, \max} = G_{cr}. \quad (10)$$

On the other hand, Anderson et al [4] have obtained  $G_{\theta, \max}$  by using the total energy method proposed by Dixon and Pook [6]. In this method, when a crack propagates by an infinitesimal length,  $\Delta a$ , in an arbitrary direction,  $\theta$ , from the original crack tip under a constant load, one half of the external work during the propagation of the crack is equal to the amount of  $G_\theta$ , that is,

$$G_\theta = \frac{1}{2} \sum_{i=1}^n \frac{P_i \Delta \delta_i}{\Delta a} \quad (11)$$

where

- $P_i$  : external load vector acting at the point  $i$
- $\Delta \delta_i$  : change in displacement of the point  $i$  as the crack propagates by an infinitesimal length,  $\Delta a$
- $n$  : number of points where the external loads are applied.

#### EXPERIMENTAL PROCEDURES

Two kinds of test specimens are shown in Figure 2. One is the cruciform type and the other is straight side. Each one contains a centre notch which is machined through thickness, and is inclined at an angle,  $\beta$ , to the vertical direction. The fracture tests of PMMA were conducted at room temperature. For these tests, a 100 kN vertical testing machine which was controlled by displacement was employed for one direction, and for the other one, a load was applied by specially designed screw-type loading apparatus.

The test of SM41 were performed at approximately constant temperature of  $-140^\circ\text{C}$  which results in brittle fracture of the specimens with a small scale yielding. This small scale yielding condition at  $-140^\circ\text{C}$  was confirmed by the notched wide plate test or the deep notch test. A 3,000 kN vertical testing machine was used, with a special designed 1,500 kN horizontal testing machine which can move during testing in accordance with the vertical displacement of the specimen. In order to examine the stress distribution in the cruciform specimens, strains in the specimen were measured by means of strain gages.

## TEST RESULTS AND DISCUSSION

Stresses Surrounding the Notch

It is necessary to know the stresses on the specimens at fracture, in order to compare the observed fracture stress and the direction of initial crack propagation with those predicted by the three criteria mentioned above. According to both the results of a stress analysis by using the finite element method and the measured ones, the average stresses in the central portion of the cruciform specimens,  $\sigma_{ex}$  and  $\sigma_{ey}$ , are expressed with the average stresses at the loading edges,  $\sigma_x$  and  $\sigma_y$  in the matrix form as follows:

$$\begin{pmatrix} \sigma_{ex} \\ \sigma_{ey} \end{pmatrix} = \begin{bmatrix} 0.80 & -0.09 \\ -0.09 & 0.80 \end{bmatrix} \begin{pmatrix} \sigma_x \\ \sigma_y \end{pmatrix} \quad (12)$$

Also, it is necessary to consider the effect of finite width of specimens. However, the correction factor of the finite width for the stress intensity factor is at maximum 1.07, by employing the Irwin's tangent formula. These correction factors are small, and their effects are ignored in the following discussion.

Characteristics of Brittle Fracture on PMMA Specimens

The test results from 83 PMMA specimens including the cruciform and straight side ones are summarized in Figures 3 and 4. In Figures 3a, 3b and 3c, the direction of initial crack propagation is plotted against the crack angle,  $\beta$ , for the load ratios of 0/1, 1/2 and 1/1, respectively. The curves in these figures are those predicted by the three criteria mentioned above. When the load ratio is 1/1, the fracture angle curves obtained from  $\sigma_{\theta, \max}$  criterion and  $S_{\min}$  criterion coincide with each other, and are represented with one curve ( $-\theta_0 = 0^\circ$ ). When the load ratio is 1/1, the direction of initial crack propagation almost coincides with the original crack line ( $-\theta_0 = 0^\circ$ ). In the case of load ratio, 1/2, the fracture angle,  $-\theta_0$ , is shown to be between those in the case of the load ratios, 0/1 and 1/1. In Figures 4a, 4b and 4c, the fracture stresses are plotted against the crack angle,  $\beta$ , by normalizing with respect to fracture stresses when  $\beta$  is  $90^\circ$ , which show almost same values regardless of load ratios. The load ratios in Figures 4a, 4b and 4c are 0/1, 1/2 and 1/1, respectively. The theoretical curves in these figures are also obtained from these criteria. In the case of load ratio, 0/1, the fracture stresses increase. When the load ratio is 1/2, the fracture stresses also increase as  $\beta$  decreases, but do not exceed 2.4 times of that for  $\beta$  of  $90^\circ$ . The fracture stresses at the load ratio equal to 1/1 show nearly identical value to that for  $\beta$  of  $90^\circ$ . From the test results in case of  $\beta = 90^\circ$ , no influence can be observed on the fracture stresses with respect to the stresses parallel to the crack direction. In the following, the three criteria mentioned above are discussed in comparison with the test results.

 $\sigma_{\theta, \max}$  Criterion

The test results in this paper are in good agreement with the curves obtained from  $\sigma_{\theta, \max}$  criterion when  $\alpha$  is 0.1 ( $r_c = 0.1$  mm). As known from

the above discussion, the stresses parallel to the crack direction have a significant effect both on the direction of initial crack propagation and the fracture stress, according to this criterion. However, the physical meaning of  $r_c$  of 0.1 mm is not clear.

 $S_{\min}$  Criterion

The curves obtained from  $S_{\min}$  criterion are in good agreement with the test results except the direction of initial crack propagation when the load ratio is 1/2. However, the physical meaning of this criterion is not understood.

 $G_{\theta, \max}$  Criterion

Judging from curves in Figures 3 and 4,  $G_{\theta, \max}$  criterion predicts fairly accurately the direction of initial crack propagation and the fracture stresses obtained from the tests in this study. It is known that  $G_{\theta, \max}$  criterion is the most suitable in studying brittle fracture characteristics under the mixed mode stress system. In this study,  $G_{\theta}$  can be calculated numerically by using the finite element method.

Characteristics of Brittle Fracture on SM41 Specimens

The predictions obtained from  $G_{\theta}$  analysis by applying the finite element method are in good agreement with the test results as to the direction of initial crack propagation. However, there are some differences between them as far as the fracture stresses are concerned, in particular these differences are most predominant when the angle,  $\beta$ , is  $45^\circ$ . To study these differences, the critical decreasing rate of total potential energy,  $G_{cr}$ , are plotted in Figure 5 against the mode II stress intensity factor  $K_{II}$ , by applying the results of  $G_{\theta}$  analysis obtained by the finite element method. The same results of PMMA specimens are also shown in this figure. In the case of PMMA, which is elastic and perfectly brittle, the slip does not occur, and the energy stored in the core region surrounding the crack tip due to the mode II deformation is completely dissipated at fracture. Therefore, the value of  $G_{cr}$  does not show dependency on  $K_{II}$  value. On the other hand, in the case of SM41, the stored energy is partly dissipated in forming slip lines. In the ordinary elastic-plastic material such as SM41, the slip lines form at an angle of  $45^\circ$  to the directions of principal stresses. Consequently, the in-plane shear deformation under mode II stress system causes this slip most effectively when the direction of slip lines coincide with the original crack direction,  $\beta = 45^\circ$ . This phenomenon is considered one of the main reasons why the critical value of decreasing rate of total potential energy,  $G_{cr}$ , increases as the value of  $K_{II}$  increases as shown in Figure 5.

## CONCLUSIONS

The following conclusions can be drawn from this study.

- (1) The criterion of maximum decreasing rate of total potential energy is very suitable in predicting the brittle fracture stress and the direction of initial crack propagation under a mixed mode stress system of modes I and

11, which is a combination of the opening and in-plane shear modes.

(2) In the case of the load ratio of 1/2, the fracture stress increases up to 2.4 times that for  $\beta = 90^\circ$ , as the inclination angle of notch to the direction of the main load,  $\beta$ , decreases.

(3) In the case of the load ratio of 1/1, which is equivalent to uniform tension in all directions, the fracture stress does not vary with  $\beta$ , and the direction of initial crack propagation coincides with the line of notch.

(4) In the case of the load ratio of 0/1, that is, the uni-axial load, the fracture stress increases as  $\beta$  decreases. However, the direction of initial crack propagation is almost normal to the loading direction irrespective of  $\beta$ .

(5) The uniform stress applied parallel to the line of notch has little effects on the direction of initial crack propagation and the fracture stress.

(6) In the case of an elastic-plastic material such as SM41, the energy stored in the core region surrounding the crack tip is partly dissipated in forming slip lines, and the critical value,  $G_{cr}$ , increases as  $K_{II}$  value derived from the in-plane shear deformation increases. On the other hand, in the case of elastic and perfectly brittle material such as PMMA, this stored energy is completely dissipated at fracture, and the critical value,  $G_{cr}$ , does not show the dependency on  $K_{II}$  value.

#### ACKNOWLEDGEMENTS

The authors wish to express their thanks to Professor T. Kanazawa and the members of Welding Research Committee, the Society of Naval Architects of Japan, for their helpful discussions. The authors highly appreciate the support offered by Professor Emeritus H. Kihara, Professor K. Satoh and Associate Professor M. Toyoda for the installation of the bi-axial tensile testing machine of 3,000 kN.

#### REFERENCES

1. ERDOGAN, F. and SIH, G. C., Trans. ASME, J. of Basic Eng., 85, 1963, 519.
2. WILLIAMS, J. G. and EWING, P. D., Int. J. Frac. Mech., 8, 1972, 441.
3. SIH, G. C., Eng. Frac. Mech., 5, 1973, 365.
4. ANDERSON, G. P., RUGGLES, V. L. and STIBCR, G., Int. J. Frac. Mech., 7, 1971.
5. COTTERELL, B., Int. J. Frac. Mech., 2, 1966, 526.
6. DIXON, I. R. and POOK, L. P., Nature, 224, 1969.

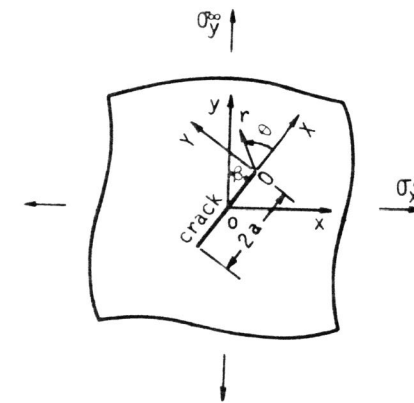


Figure 1 Stress Systems

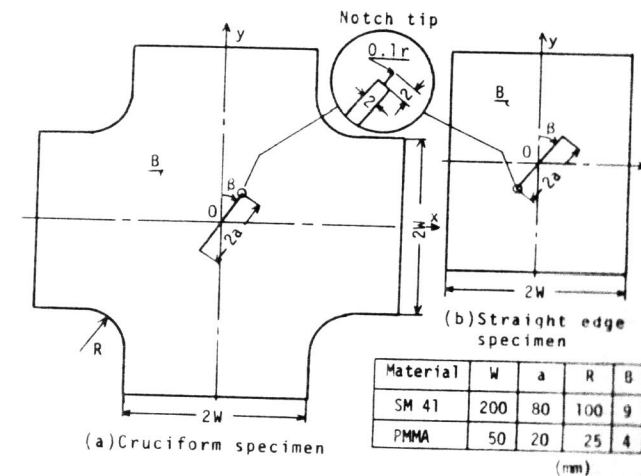


Figure 2 Details of Test Specimen

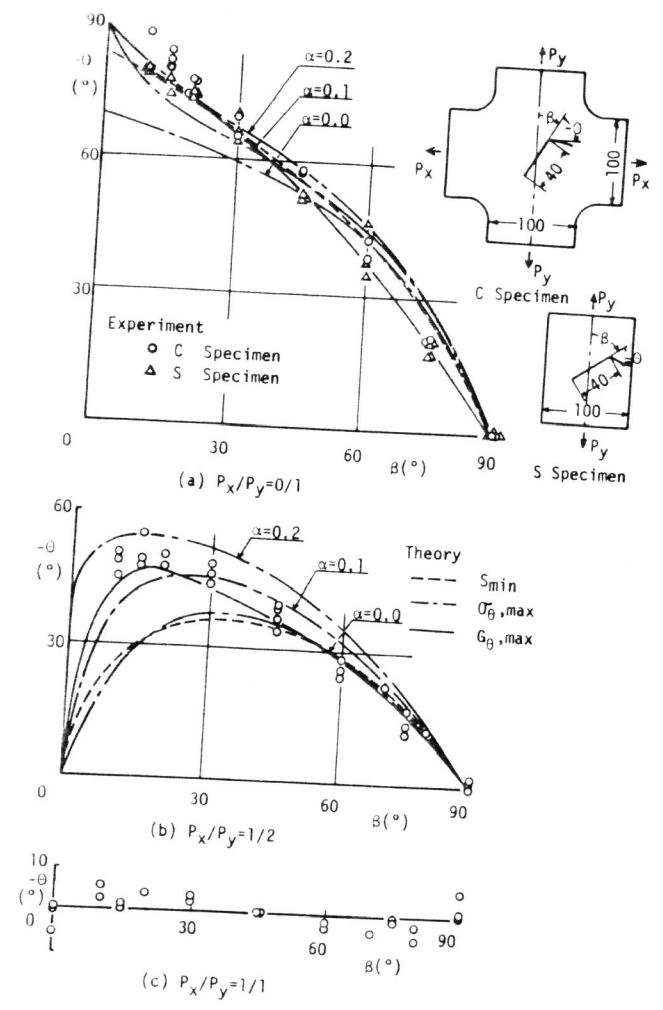


Figure 3 Direction of Crack Propagation (PMMA)

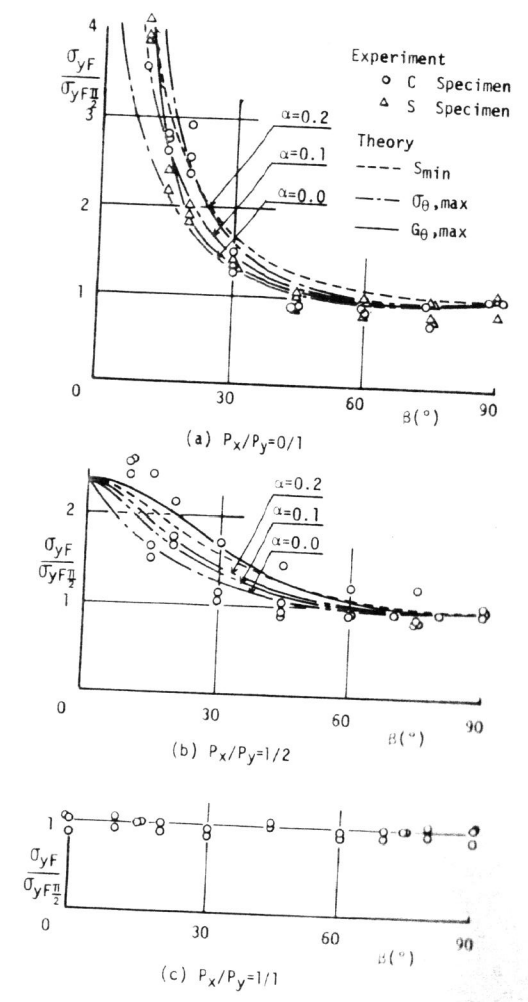


Figure 4 Fracture Stresses Non-Dimensionalized by Fracture Stress of Specimen of  $\beta = 90^\circ$  (PMMA)

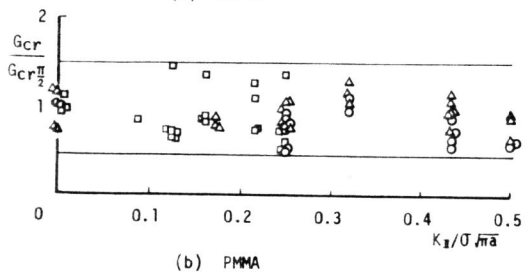
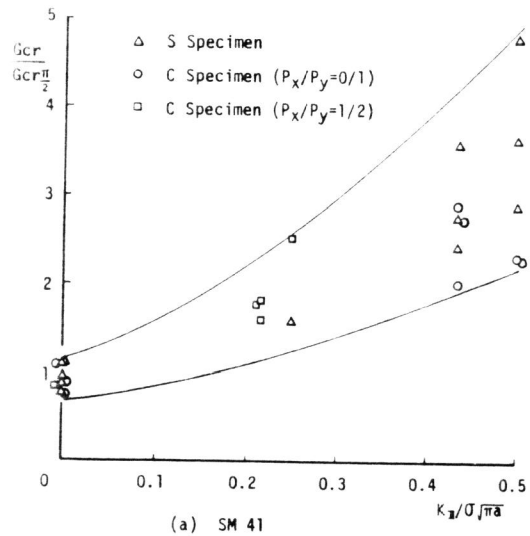


Figure 5 Variation of Critical Decreasing Rate of Total Potential Energy with  $K_{II}$